



**Florence DAYS – 5<sup>th</sup> – 6<sup>th</sup> June, 2013**

**Paper 2013-18**

**Determining the a.c. corrosion risk of pipelines based on coupon measurements**

**Ermittlung des Risikos der Wechselstromkorrosion für Rohrleitungen auf der Grundlage von Messungen an Probeblechen**

**Détermination du risque de corrosion C.A. de canalisations sur la base de mesures de coupons**

M. Büchler, SGK Swiss Society for Corrosion Protection,  
Technoparkstr. 1, CH-8005 Zürich,  
markus.buechler@sgk.ch

## **Abstract**

Most of the knowledge gained on a.c. corrosion was obtained by means of coupon measurements. They allowed building a profound understanding of the relevant parameters, explaining their significance as well as the corresponding threshold values based on thermodynamic and kinetic concepts. The corrosion rates derived from the theoretical models are often confirmed by coupon measurements, demonstrating the validity of the concepts as well as the corresponding measuring techniques. However, the significant corrosion rates obtained on coupons are typically not observed on pipeline systems. The reasons for this discrepancy are addressed by means of theoretical considerations and numerical simulations. The obtained results are compared with field data. Based on the good agreement between calculation and experimental data a new approach to assessing the a.c. corrosion risk is proposed that is based on the current threshold values of FprEN 15280.

## **Zusammenfassung**

Das heutige Verständnis bezüglich Wechselstromkorrosion wurde größtenteils mit Hilfe von Probestreifen gewonnen. Diese ermöglichten es, die relevanten Parameter sowie deren Bedeutung zu ermitteln und die Grenzwerte mit Hilfe von thermodynamischen und kinetischen Konzepten zu erklären. Die aufgrund der Modellvorstellungen erwarteten Korrosionsgeschwindigkeiten wurden bei Messungen an Probestreifen sowohl im Labor als auch in Feldversuchen oft bestätigt. Die praktische Erfahrung zeigt aber, dass die Korrosionsgeschwindigkeiten an Rohrleitungssystemen meist deutlich geringer sind als die aufgrund der Modellvorstellungen und den an Probestreifen ermittelten Werten. Die Gründe für diese Diskrepanz werden mit Hilfe von Berechnungen und dem Vergleich mit Felddaten analysiert. Basierend auf der guten Übereinstimmung wird ein neuer Ansatz für die Bewertung der Wechselstromkorrosionsgefährdung von Rohrleitungen basierend auf den Grenzwerten der FprEN 15280 vorgeschlagen.

## **Résumé**

La majorité des connaissances acquises en matière de corrosion C.A. ont été obtenues grâce à des mesures de coupons. Ces mesures ont permis d'acquérir une compréhension approfondie des paramètres pertinents, expliquant leur importance ainsi que les valeurs seuils correspondantes basées sur des concepts thermodynamiques et cinétiques. Les taux de corrosion déduits des modèles théoriques sont souvent confirmés par les mesures de coupons, démontrant ainsi la validité des concepts ainsi que les techniques de mesure correspondantes. Cependant, les taux de corrosion importants obtenus sur les coupons ne sont généralement pas observés dans les réseaux de canalisations. Les raisons de ce décalage sont abordées par le biais de considérations théoriques et de simulations numériques. Les résultats obtenus sont comparés aux données de terrain. Sur la base de la bonne concordance entre calcul et données expérimentales, une nouvelle approche pour l'évaluation du risque de corrosion C.A. est proposée, laquelle est basée sur les valeurs seuils de FprEN 15280.

## 1. Introduction

In 1988, the first damages by alternating current (ac) corrosion of cathodic protected pipelines have been observed [1, 2]. As a result, this type of corrosion was investigated and soon the ac current density ( $J_{ac}$ ) was identified as the critical parameter [3-5]. Later the influence of the protection current density ( $J_{dc}$ ) on the corrosion rate was reported [6-9]. A deeper understanding of the processes involved has been missing for a long time though. Only recently, a model was developed that is able of explaining the empirical observations [10-13]. In recent years extensive work has been performed in order to obtain a more profound understanding of the involved mechanisms and methods for mitigation.

Based on the obtained results, the corrosion rate can be reduced to a negligible level when the protection current density is limited [7, 14]. Preferably, it should be less than  $1 \text{ A/m}^2$ . This should be achieved if the on-potential ( $E_{on}$ ) is in the range of  $-1.2 \text{ V CSE}$  and the average ac voltage ( $U_{ac}$ ) is below  $15 \text{ V}$  [15, 16]. Additionally, the IR free-potential ( $E_{IR-free}$ ) must be more negative than the protection criterion according to EN 12954. Under these conditions, the driving voltage for the direct current flow is minimized, which reduces the risk of ac corrosion to a significant extent.

Based on the model concepts and experimental data ac corrosion can also be prevented at high  $J_{dc}$ . Based on laboratory tests it is likely that this is possible when  $J_{dc}$  is larger than one third of  $J_{ac}$  [6, 15].

Although there was a profound understanding of the involved processes in ac corrosion and the required thresholds [17, 18], it was not clear whether these can be effectively applied to pipelines or whether operational constraints make their implementation impossible. Therefore, extensive field test were carried out [19]. Thereby the relevance of the laboratory tests for field application was investigated. The thresholds found in laboratory investigations could be confirmed and some of these values could be explained based on thermodynamic and kinetic data.

Interestingly the corrosion rates observed on coupons in field tests are typically significantly larger than the corrosion rates observed on Pipelines [20]. This can be illustrated by the repeated perforation of coupons with a thickness of  $1 \text{ mm}$  within one year due to a.c. interference, while the pipeline with a wall thickness of  $5 \text{ mm}$  is in operation for several decades under the very same operation conditions without any leakages. These observations could lead to the conclusion that the threshold values elaborated on coupons are too strict. In contrast, coupon measurements in low resistive soil indicate that the current threshold values should even further be restricted.

These observations are explained based on mathematical description of the mutual dependency of d.c. and a.c. currents.

## 2. Calculations

### 2.1. Introduction

The various strategies for optimizing the cathodic protection on a.c. interfered pipelines are described in [21]. Additionally to the threshold values based on current densities, which can only be determined on coupons, criteria with respect to the on-potential and the a.c. voltage were introduced (Fig. 1) that can readily be determined at each test post.

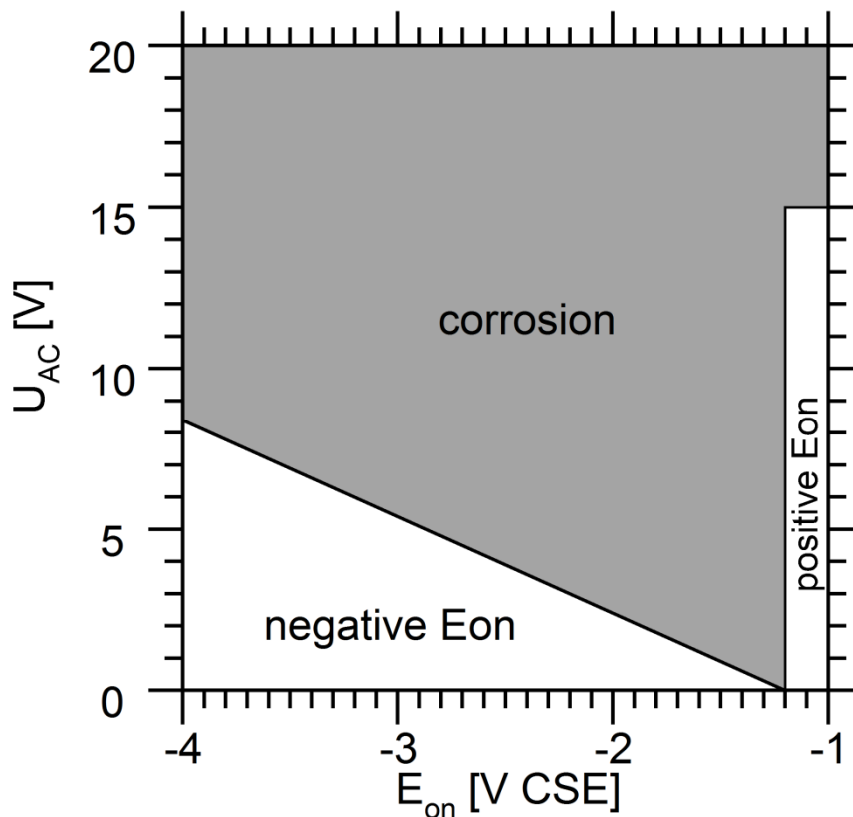


**Fig. 1:** Threshold values for a.c. voltage and on-potential for the protections strategies at positive and negative on-potential. Corrosion has to be expected when the values are in red field.

Based on Fig. 1 the potential range for operating the cathodic protection at positive on-potential is narrow. This results in high requirements regarding the operation of the rectifier. Since the results obtained on coupons in low resistive soil indicate that the threshold values might even be more restrictive [22], the applicability of the protection at positive on-potential is questionable. In contrast, it is observed that the corrosion rate on pipelines is smaller than the one measured on coupons, which could justify an increase of the protection domain to more negative on-potentials. As a consequence, the mutual dependence of the various parameters on-potential and d.c. current density as well as a.c. voltage and a.c. current density was described based on a mathematical model, that is derived from field data [19].

## 2.2. Calculation model

The protective d.c. current density  $J_{dc}$ , which enters the steel of a pipeline in a coating defect with an area  $A$ , can be calculated from the spread resistance  $R$  of the defect and from the difference between the on-potential ( $E_{on}$ ) and the IR-free potential ( $E_{IR-free}$ ) of the steel in the defect according to equation (1). With values of  $E_{on}$  more positive than  $-1.2 V_{CSE}$ , it was found [13] that  $J_{dc}$  can converge towards zero. Therefore, it is possible in many cases to limit a.c. corrosion even in the case of increased a.c. interference, by controlling  $E_{on}$ .

$$J_{dc} = \frac{E_{IR-free} - E_{on}}{R \cdot A} \quad (1)$$

However, it is well known that an a.c. current passing through the steel surface in a coating defect can cause an anodic shift of  $E_{IR-free}$  according to equation (2), where  $\Delta E_F$  is the contribution of this faradaic rectification [23] and  $E_p$  is the effective polarization of the steel surface that would be present at the given  $J_{dc}$  in absence of a.c. interference.

$$E_{IR-free} = E_p + \Delta E_F \quad (2)$$

The evaluation of literature data [15, 24] with respect to the a.c. current density and the resulting anodic shift of  $E_{IR-free}$  follows the relationship shown in Fig. 2.

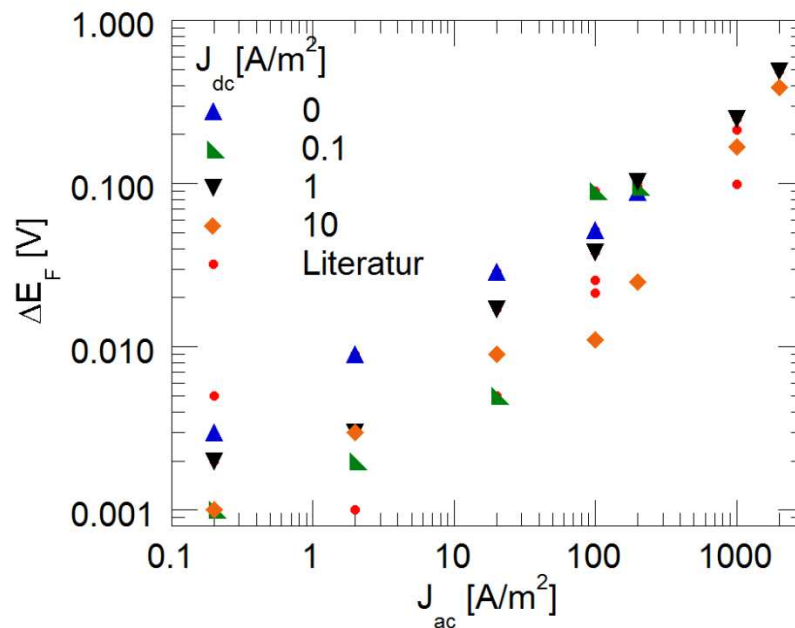


**Fig. 2:** Dependence between anodic shift of  $E_{IR-free}$  and  $J_{ac}$  in 0.01 M NaOH according to [15]. The values from reference [24] are determined in sulfate solution.

By means of linear regression with an assumed empirical relationship according to equation (3) the proportionality factor  $f$  can be found at  $0.21 [mV \cdot m^2/A]$ .

$$\Delta E_F = f \cdot \frac{U_{ac}}{R \cdot A} \quad (3)$$

$$U_{ac} = R \cdot A (J_{dc} \cdot R \cdot A - E_p + E_{on}) / f \quad (4)$$

Hence equation (4) describes the dependence of the on-potential and the acceptable a.c. voltage as a function of the critical  $J_{dc}$ .

### 2.3. Discussion of the results

Assuming a value of  $-1.2 \text{ V}_{\text{CSE}}$  for  $E_p$ , a circular defect with the surface  $A$  according to equation (5), its spread resistance  $R$  according to equation (6), and a critical protection current density  $J_{dc}$  of  $1 \text{ A/m}^2$  the dependence shown in Fig. 3 is obtained as a function of various on-potentials. Additionally the limiting conditions for  $J_{ac}$  of  $30 \text{ A/m}^2$  and  $J_{ac}/J_{dc}$  of 3 are calculated.

$$A = \pi \frac{d^2}{4} \quad (5)$$

$$R = \frac{\rho}{2 \cdot d} \quad (6)$$

It can be concluded that the threshold for a.c. corrosion according to Fig. 1 is only valid for increased soil resistivity. In the case of low values, as they can be found in clay, sea water, or sea water soaked soil, a.c. corrosion has to be expected at a.c. voltages below  $15 \text{ V}$  and at on-potentials of  $-1.15 \text{ V CSE}$ . Hence, the corrosion observed under certain conditions in practical application, while meeting the requirements of Fig. 1, can be explained qualitatively by means of equation (4) and the contribution of the low soil resistivity.

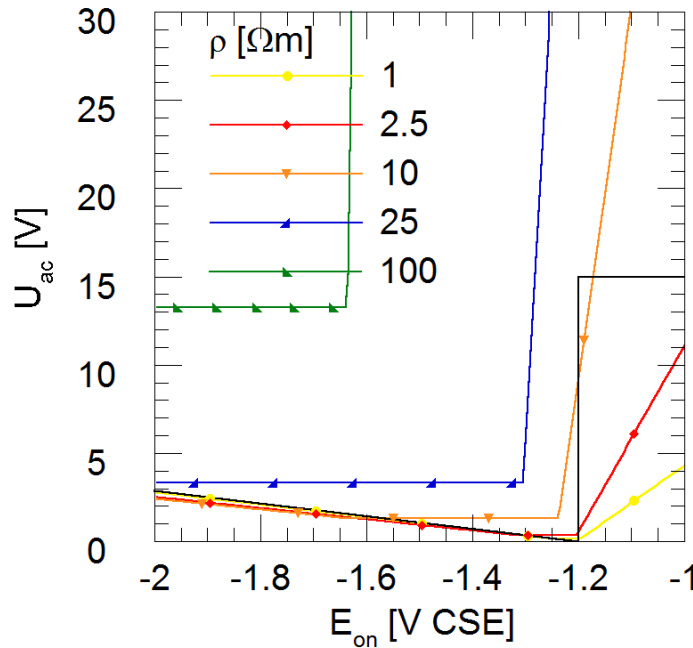
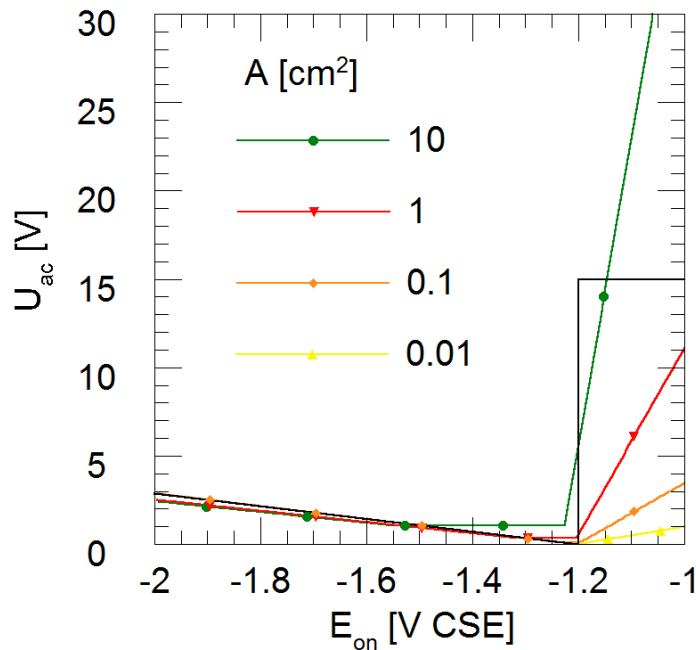


Fig. 3: Dependence of  $U_{ac}$  on  $E_{on}$  at various soil resistivities and a defect surface of  $1 \text{ cm}^2$  according to equation (4). In black the thresholds from Fig. 1 are shown.



**Fig. 4:** Dependence of  $U_{ac}$  and  $E_{on}$  at various defect sizes at a soil resistivity of  $2.5 \Omega m$  according to equation (4). In black the thresholds from Fig. 1 are shown.

In the discussion of equation (4) it is assumed that the spread resistance of a defect is not influenced by  $J_{dc}$ . This is true in the case for very low soil resistivity [25]. The calculation of the effect of the defect surface  $A$  on the critical  $U_{ac}$  is shown in (Fig. 4). Clearly, the acceptable  $U_{ac}$  decreases strongly with decreasing surface. Hence, a.c. corrosion always has to be expected on pipelines even at very low  $U_{ac}$ . The current density occurring on a defect is additionally influenced by the thickness of the adjacent coating. The ohmic potential drop in the pore results in an increase of the acceptable  $U_{ac}$  and can compensate part of the negative effect of the low resistive soil.

When the critical  $U_{ac}$  is exceeded, a.c. corrosion can occur with significant corrosion rates in the range of up to 100 mm/year. The corrosion process is bound to result in an increase of the defect surface according to Fig. 6. While the surface increases, the diameter of the defect remains constant, at least in the case of stable PE coatings with several millimeters thickness. Hence, the spread resistance and therefore the currents remain approximately constant, but the current densities decrease with increasing corrosion depth. The influence of the corrosion depth on a coating defect with 1 mm diameter and 1 mm coating thickness is shown in Fig. 5 for an assumed hemispherical corrosion attack in Fig. 6. The deeper the corrosion pit the higher is the acceptable  $U_{ac}$  at a given  $E_{on}$ .

This observation has direct consequences on the a.c. corrosion on pipelines. It has to be expected that a variety of defect diameters will be present on a pipeline including defects smaller than  $1 \text{ cm}^2$ . Therefore, critical  $J_{ac}$  and  $J_{dc}$  have to be expected. According to Fig. 4 corrosion will take place. With increasing corrosion process the surface of the defect and also the critical  $U_{ac}$  are increased. According to Fig. 5 the corrosion process is expected to slow down and eventually come to a stop. This qualitative observation has direct consequences for the use of coupons, since they are typically significantly thinner than the pipeline wall thickness. Commercially available products have thicknesses in the range of 0.1 to 1 mm. The corrosion

depth and therefore the surface increase cannot reach significant values. This effect is schematically shown in Fig. 6. As soon as the coupon is perforated, the surface of small coupons will get smaller with increasing corrosion process (Fig. 6a3), increasing the current densities and thus the susceptibility to ac corrosion. In contrast, on the thicker pipeline the exposed steel surface will further increase (Fig. 6b3) and the corrosion process can be expected to slow down or even stop.

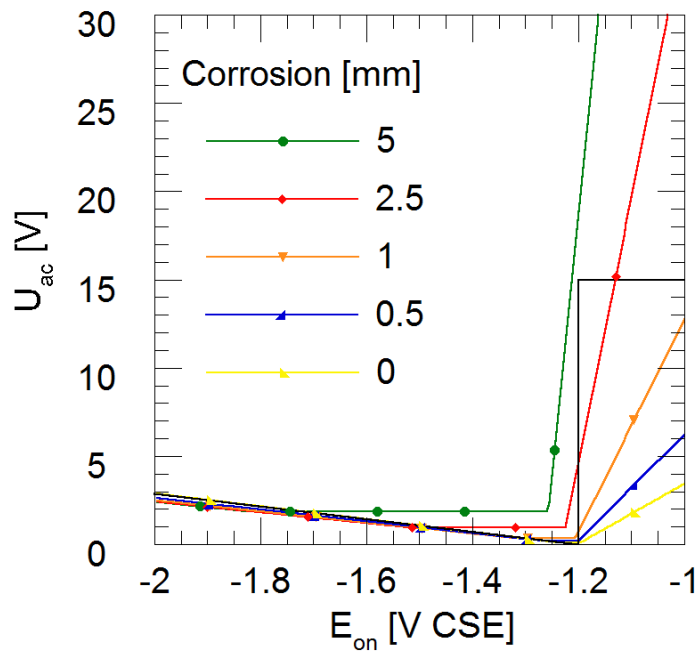


Fig. 5: Dependence of  $U_{ac}$  and  $E_{on}$  at various corrosion depths and a coating thickness of 1 mm, at a soil resistivity of  $2.5 \Omega m$  and a defect surface of  $0.01 \text{ cm}^2$  according to equation (4). In black the thresholds from Fig. 1 are shown.

These considerations are a possible explanation for the general observation that the corrosion rates observed on coupons are significant and would have resulted in leaks on a given pipeline, while the pipeline does neither show leaks nor any major corrosion damage according to inline inspection tools. The discrepancy between the behavior of coupons and pipeline should be especially pronounced with very thin coupons.

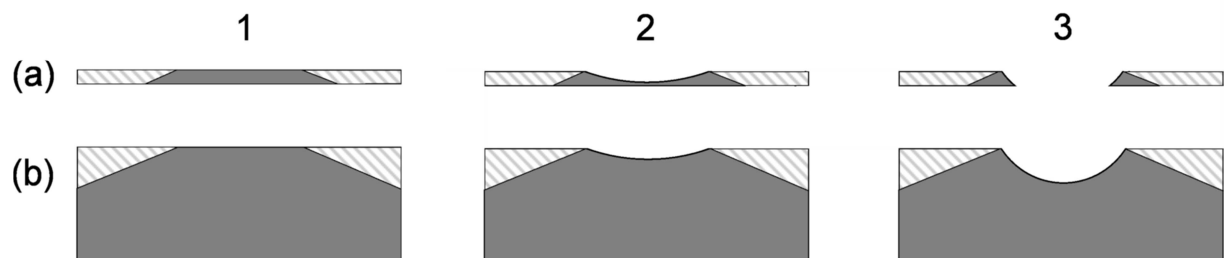


Fig. 6: Influence of the thickness of the coupon on the corrosion progress with increasing depth (1 to 3): a) thin coupon, b) thick coupon.

The calculation according to equation (4) allows a new view on the corrosion damages on pipelines. It can be concluded that a.c. corrosion always has to be expected on small defects. Moreover it is expected that the initial corrosion rate is high and may be in the range of the theoretically expected 70 mm/year [15]. With increasing depth of the corrosion and therefore



increasing surface it may be expected that the corrosion rate will slow down and eventually reach a value of zero.

If these considerations are correct, the measurement of the corrosion rate on thin coupons will primarily reflect the situation of the initial stages of the corrosion process. The results should depend on the geometrical configuration and especially on the surface of the coupon. Moreover it may be expected that the corrosion rate will slow down over time. This conclusion is especially true for the coupon that repeatedly perforated within a year and that was therefore not able to describe the corrosion situation of the corresponding pipeline.

Instead of focusing on the corrosion rate, determination of the maximum acceptable corrosion depth would rather be of practical relevance. As a consequence, the thickness of a perforation coupon should correspond to this value.

## 2.4. Extension of the model

By considering also the relevant thermodynamic [26] and kinetic [27, 28] parameters of steel as well as a mathematical description of the change of the spread resistance [25] due to an increased pH [15] at the steel surface, equation (4) allows to describe the corrosion process under a.c. interference on cathodically protected pipelines in more detail. As a consequence it is possible to calculate the critical interference values depending on the soil resistivity, the defect size and the corrosion depth.

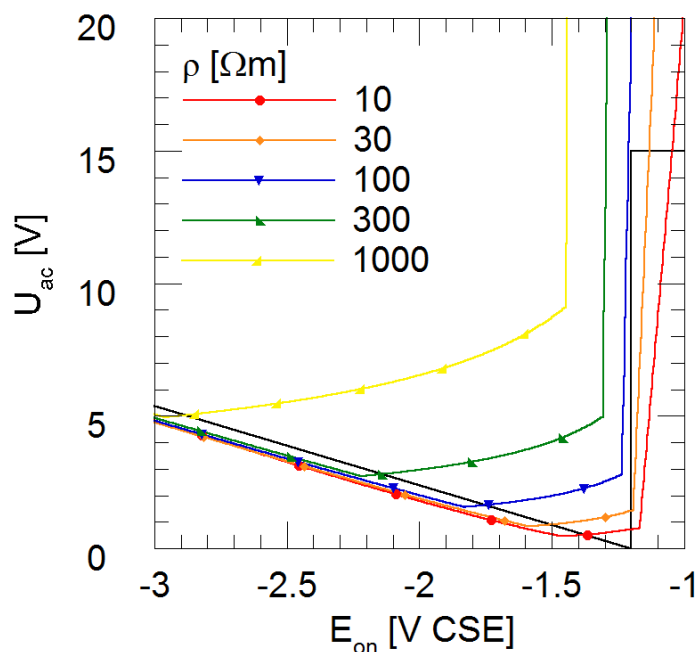


Fig. 7: Effect of soil resistivity on the thresholds for coating defects with  $1 \text{ cm}^2$ . The calculation was performed under consideration of the thermodynamic, the kinetic, and the mass transport.

The results for various soil resistivities are shown in Fig. 7. Compared to the data in Fig. 3, the curves are shifted to more positive  $E_{on}$ . This is due to the consideration of the increase of pH at the steel surface and the therefore decreased spread resistance of the defect.

The data confirm the observation that the threshold values for  $U_{ac}$  may be lower than those shown in Fig. 1 in the case of low soil resistivity. The corresponding field data can, therefore, be

explained. In contrast, at increased soil resistivity more negative values of  $E_{on}$  are acceptable. Additionally, based on the calculation model, even elevated a.c. voltages could be tolerated for the given conditions.

Considering the data in Fig. 4, it can be concluded that the acceptable  $E_{on}$  at a given  $U_{ac}$  shifts to more positive values with decreasing defect surface. This also has to be expected in the case of partial formation of calcareous deposits or heterogeneous current distribution, which leads to inhomogeneous corrosion attack. Hence, if coating defects smaller than  $1 \text{ cm}^2$  are expected, the threshold values should be more restrictive. In contrast, more negative  $E_{on}$  or higher  $U_{ac}$  can be tolerated when a certain corrosion depth is tolerated. Based on the currently available information the considerations of various defect sizes in combination with a tolerable corrosion depth could lead to threshold values that are in the range of those shown in Fig. 1, but with significantly increased tolerable  $U_{ac}$ . This conclusion will have to be verified with thick coupons in field and laboratory tests.

## 2.5. Comparison of the extended model with field data

Since the model provides a full description of the processes taking place in a single coating defect, it can readily be used for describing data collected in extensive field tests [19]. The complete availability of all necessary parameters allows the direct calculation of the specific critical interference conditions. The advantage of the thermodynamic-kinetic description of the processes will be discussed based on the results in Fig. 8 and Table 1.

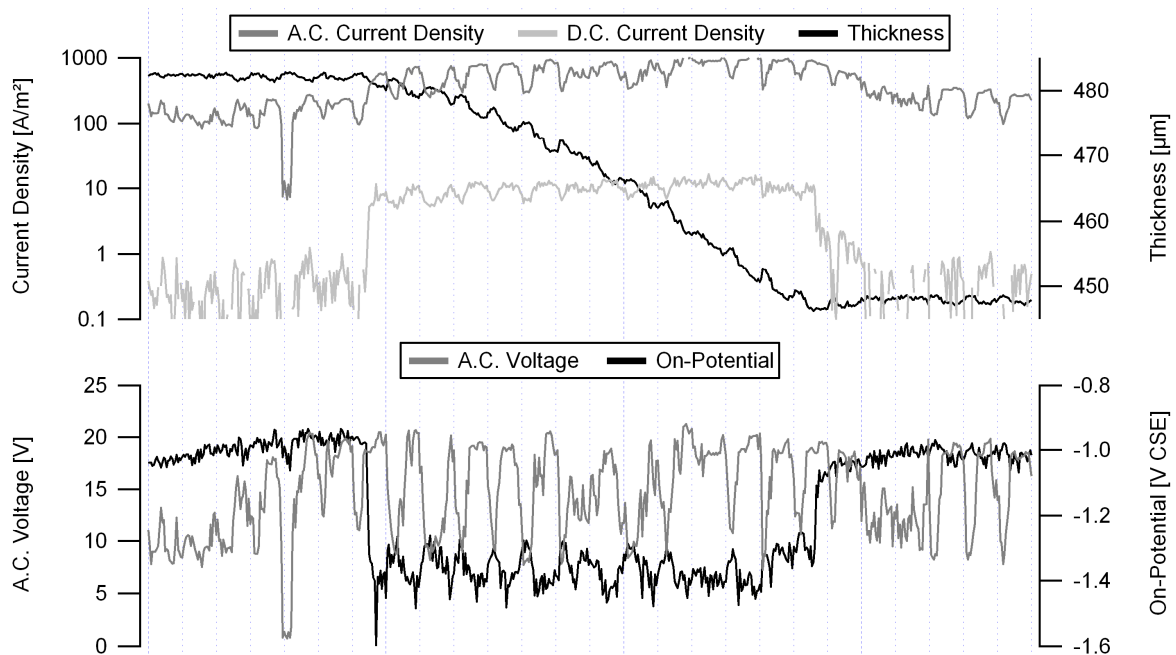


**Fig. 8:** Variation of the current densities, the coupon thickness,  $E_{on}$  and  $U_{ac}$  at a field location determined by means of ER-coupons [19].

In Fig. 8 the results determined at a field site by means of ER-coupons with a surface of  $1 \text{ cm}^2$  are shown. At this location the soil resistivity is  $13.7 \Omega\text{m}$  and the average  $U_{ac}$  is approximately 15 V. Based on these data and an average  $E_{on}$  of -1.4 as well as -1.0 V CSE, the current densities in Table 1 are calculated. The comparison with the field data shows a relatively good agreement. Additionally, the pH-value,  $E_{IR-free}$  and the potential relevant for cathodic protection, i.e.  $E_p$ , are calculated (Table 1). This demonstrates clearly that with equation (4) in combination

with thermodynamic and kinetic parameters as well as with mass transport considerations, a far reaching description of the involved parameters is possible.

**Table 1: Parameters calculated for the coupon shown in Fig. 8**

$E_{on}$ [V <sub>CSE</sub> ]	$U_{ac}$ [V]	$J_{dc}$ [A/m <sup>2</sup> ]	$J_{ac}$ [A/m <sup>2</sup> ]	pH	$E_{ir-free}$ [V <sub>CSE</sub> ]	$E_p$ [V <sub>CSE</sub> ]
-1.4	15	15.3	911	13.2	-1.15	-1.34
-1.0	15	0.34	412	12.2	-0.99	-1.07

The threshold values calculated for the specific conditions in the field test in Germany are shown in Fig. 9 for various soil resistivities. In all cases the model calculation is capable of identifying the critical conditions.

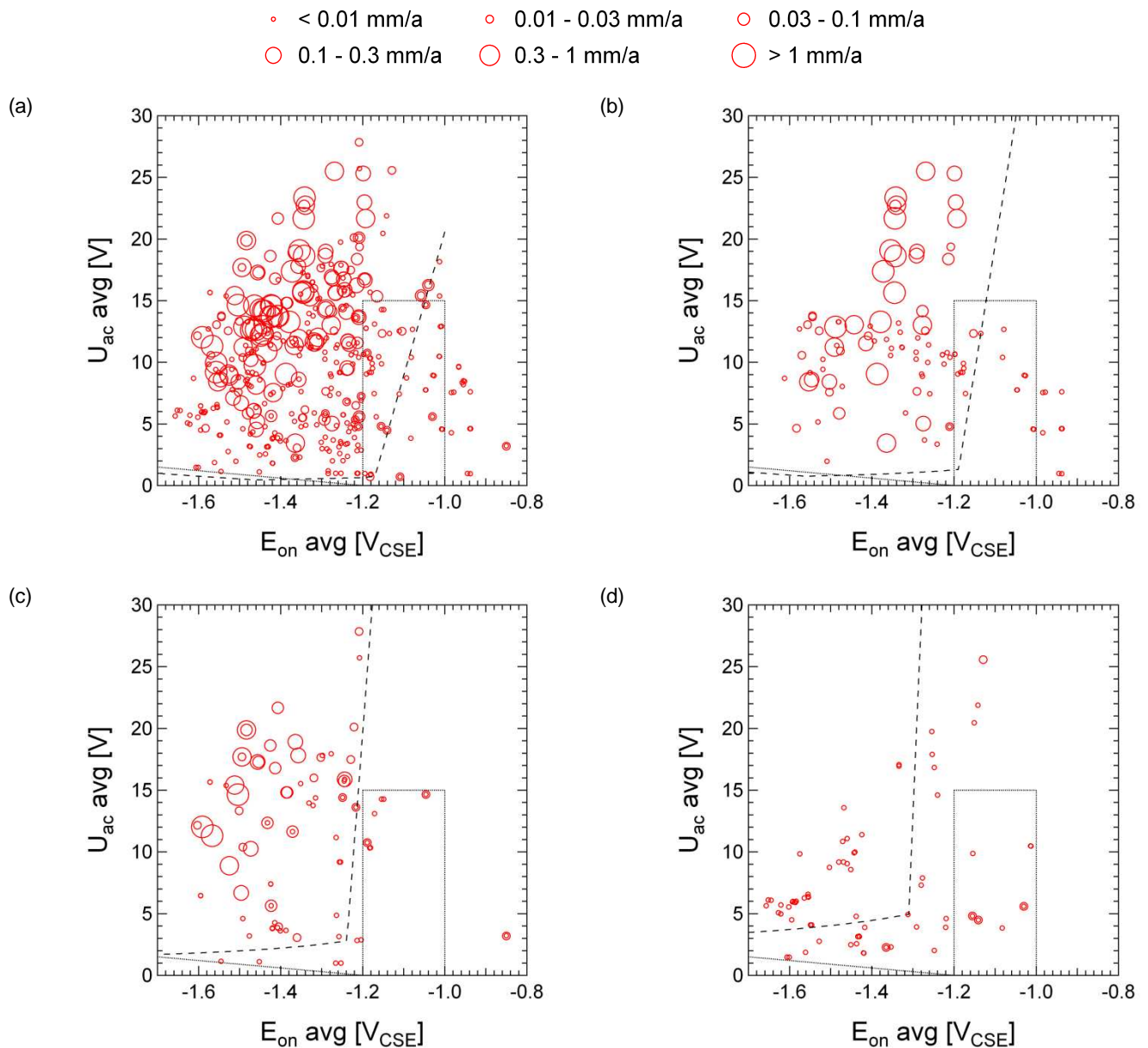


**Fig. 9:** Data from the field test on various pipelines [19] sorted according to soil resistivity. The thresholds (dashed line) were calculated for the lowest soil resistivity value: a) > 10 Ωm; b) 25 – 100 Ωm; c) 100 – 300 Ωm; d) > 300 Ωm

In the discussion of these results it has to be considered that the calculation of the threshold was made for the worst case situation. These include the assumption that anaerobic conditions are present, that no corrosion is accepted on the 1 cm<sup>2</sup> surface, that the thickness of the adjacent coating is zero, that the current flow in soil is based on hydroxide migration, and that no insulating deposits are formed on the steel surface. The corrosion behavior can be better if the following effects are considered in the calculation:

- The partial neutralization of hydroxide ions in soil by means of dissolved CO<sub>2</sub>, which will result in higher spread resistance
- The presence of aerobic conditions would result in a diffusion controlled oxygen reduction, which would result in higher acceptable protection current densities
- The formation of resistive homogeneous rust and chalk layers would increase the spread resistance

It has to be assumed that these effects may occur under normal operation conditions. This explains the numerous points in Fig. 9 that do not show significant corrosion, but are in the critical area.

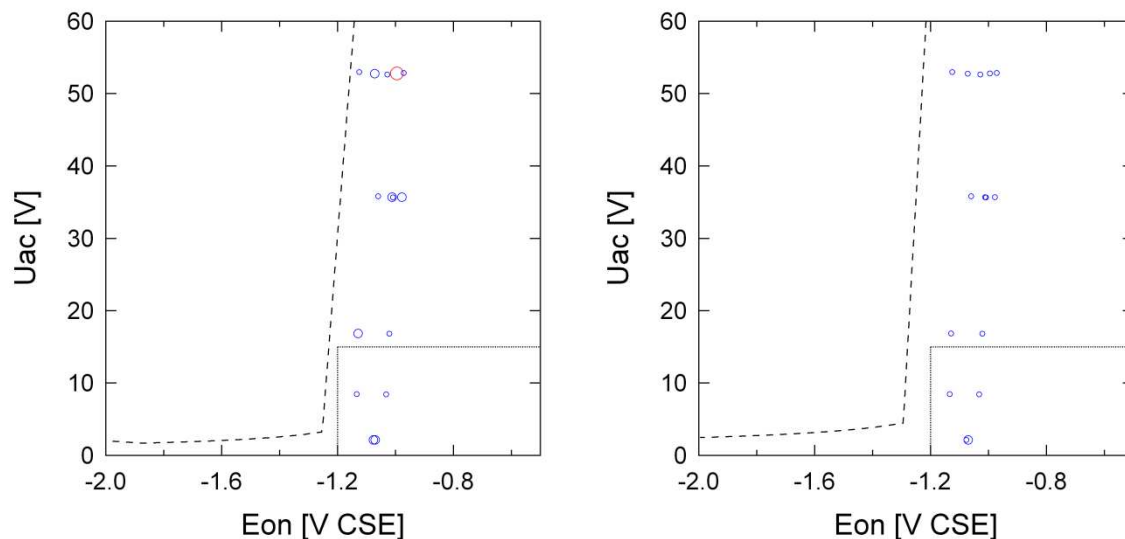


**Fig. 10:** Dependence of the corrosion rate from the average Eon and Uac determined in field tests in two different soil resistivities with ER-coupons under strong cathodic stray current interference. The legend is shown in Fig. 9. Left: 100 Ωm; right: 300 Ωm

A key conclusion from Fig. 9 is the virtually unlimited U<sub>ac</sub> that can be tolerated in the case of increased soil resistivity, large defect size, or increased acceptable corrosion depth. Most recent field investigations with strong cathodic stray current interference confirm this conclusion in the case of increased soil resistivity (Fig. 10). As long as the average Eon is sufficiently positive, no corrosion is observed even at high a.c. voltages. Only at U<sub>ac</sub> of 57 V in one instance a corrosion rate slightly higher than 30 μm/year was observed.

## 2.6. Consequences for the evaluation of the a.c. corrosion risk

The comparison of the model calculations with field data demonstrates a good agreement between the expected worst case behavior and the observed corrosion behavior for the assumption of negligible corrosion depth. This leads to direct consequences regarding the

evaluation of the a.c. corrosion risk of pipelines in the case of operation of the cathodic protection at positive on-potential.

- At soil resistivities higher than 100  $\Omega\text{m}$  and at  $E_{\text{on}}$  more positive than -1.2 V CSE a.c. voltages up to 50 V can be tolerated on the pipeline without significant corrosion on a defect with a surface  $>1 \text{ cm}^2$ .
- In the case of soil resistivities below 100  $\Omega\text{m}$  in the case of  $U_{\text{ac}}$  of up to 50 V the  $E_{\text{on}}$  must be shifted to more positive values, in order to avoid any corrosion on a defect with a surface  $>1 \text{ cm}^2$ .
- In low resistive soils below 25  $\Omega\text{m}$  at  $U_{\text{ac}}$  below 15 V and  $E_{\text{on}}$  more positive than -1.2 V CSE on defects with a surface  $>1 \text{ cm}^2$  corrosion up to a certain depth has to be expected. This corrosion can be avoided by lowering  $U_{\text{ac}}$  or shifting  $E_{\text{on}}$  to more positive values.
- In the case of defects smaller than 1  $\text{cm}^2$  corrosion has to be expected even at lower  $U_{\text{ac}}$ .
- Based on equation (4) it is expected that the corrosion will slow down with increasing depth and will even stop at a certain depth.

This discussion demonstrates that the evaluation of the corrosion risk is only possible under consideration of the soil resistivity, the average  $E_{\text{on}}$ , the average  $U_{\text{ac}}$ , the coating defect size, and the maximum acceptable corrosion depth. As a consequence at identical  $E_{\text{on}}$  a.c. voltages of 50 V can be uncritical while on different pipeline section values of 5 V can lead to corrosion depths of 10 mm.

According to equation (4) the effect of the defect surface is following a square law. Therefore the contribution of the surface is so pronounced that the corrosion process is expected to stop at a certain depth. This theoretical consideration leads to the conclusion, that a.c. corrosion leaks should be primarily observed on pipelines with a small wall thickness. The currently available information demonstrates, that so far perforation was only observed on pipelines with a wall thickness around 5 mm or less [29]. This conclusion has to be considered with caution, since the interference conditions are not known in detail in these cases. Nevertheless the observation is in line with the model calculation and the generally limited corrosion rates observed on pipelines.

The various calculations indicate that on small defect surfaces always a.c. corrosion has to be expected. This is a consequence from the pronounced influence of the defect surface according to equation (4).

Based on this discussion the currently used approach to a.c. corrosion needs some additional considerations. The use of coupons and the application of the current density criteria according to FprEN 15280 is a straightforward method to assessing the risk for coating defects with a surface of 1  $\text{cm}^2$ . However, the numerical calculations based on  $E_{\text{on}}$ ,  $U_{\text{ac}}$ , and the soil resistivities offers additional possibilities.

Starting in 2013, the effectiveness control of cathodic protection in Switzerland will be accompanied by soil resistivity measurements. Additionally the numerical calculation of various coating defect sizes at each test post will be performed and the maximum corrosion depth will be calculated. Its comparison with the tolerable corrosion depth will allow evaluating the corrosion risk. The major advantage of this procedure is to determine the possible behavior

under various hypothetical conditions without the costly installation and measurement of coupons.

### 3. Conclusions

The comparison of the model calculation with field data has demonstrated a good agreement for the worst case consideration. All results of the field test [19] could be correctly described with respect to the occurrence of corrosion.

The discussion of the various influencing parameters as well of as the model calculations allows certain conclusions that are relevant for the operation of the cathodic protection and the choice of the protection strategy:

- In low resistive soils a.c. corrosion can occur on defect surfaces of  $1 \text{ cm}^2$  even at on potentials more positive than  $-1.2 \text{ V CSE}$  and a.c. voltages of a few volts. This observation can be explained by means of the faradaic rectification of the a.c. current due to the asymmetry of the anodic and cathodic reactions. Hence, the negative effect of the a.c. current density is the increase of the d.c. current density. The corrosion can be decreased by further shifting the on-potential in positive direction.
- If the electrochemically active surface of a defect is decreased, the risk of a.c. corrosion is increased. The decrease of the corroding surface is possible due to the partial coverage with an insulating chalk layer, due to geometrically caused heterogeneous current distribution of the heterogeneous distribution of the soil resistivity. The limitation of the electrochemically active surface leads to locally increased corrosion.
- The high corrosion rates observed on thin coupons observed in field tests that are typically not found on pipelines can be explained by the strong effect of the steel surface on the corrosion process. The increase of the surface with increasing corrosion depth significantly decreases the current densities and therefore the corrosion rate over time. Based on the model calculation it may be expected that the corrosion process will stop at a certain depth.
- The thickness of coupons should be chosen in a way that the increase of the surface due to the corrosion process will be detectable. Hence the thickness of the coupon should be adjusted to the maximum acceptable corrosion depth on the pipeline.
- Current densities determined on coupons are only relevant for the given defect surfaces. Without further calculations they do not necessarily provide information with respect to the corrosion protection on smaller defect sizes.
- The geometrical modification of the defect due to the corrosion process will affect the corrosion rate over time. Hence, the extrapolation of a measured rate measured over a short period will typically lead to an overestimation of the corrosion rate. Hence the evaluation of the corrosion rate should only be made on the effectively measured time period.
- At increased soil resistivities and on-potentials more positive than  $-1.2 \text{ V CSE}$  increased a.c. voltages can be tolerated based on the model calculations. This is confirmed by most recent field tests.

It has to be considered that the final proof of the correctness of the model is still missing. However, the comparison between model calculation and available field data demonstrate a

good agreement. The model calculation is based on worst case considerations and the contribution of the electrical resistance of the corrosion products was neglected. Moreover it is typically observed that the a.c. corrosion process leads to a corrosion attack that is significantly wider than deep. Hence, the assumption of a hemispherical geometry also represents a worst case. A final model validation will only be possible by comparing the calculation with the corrosion morphology found on pipelines.

#### 4. Acknowledgement

This work was only possible due to the generous support of DVGW, Open Grid Europe GmbH, Swissgas AG, SBB AG, BFE, BAV, ERI, and Transitgas AG. A special thank goes to Hanns-Georg Schöneich for the valuable discussions and the important inputs.

#### 5. Literature

1. G. Heim, G. Peez, "Wechselstrombeeinflussung einer kathodisch geschützten Erdgashochdruckleitung", *3R International* **27**, 345 (1988).
2. B. Meier, "Kontrollarbeiten an der Erdgasleitung Rhonetal", *GWA* **69**, 193 (1988).
3. D. Bindschedler, F. Stalder, "Wechselstrominduzierte Korrosionsangriffe auf eine Erdgasleitung", *GWA* **71**, 307 (1991).
4. G. Heim, G. Peez, "Wechselstrombeeinflussung von erdverlegten kathodisch geschützten Erdgas-Hochdruckleitungen", *gwf*, 133 (1992).
5. D. Funk, W. Prinz, H. G. Schöneich, "Untersuchungen zur Wechselstromkorrosion an kathodisch geschützten Leitungen", *3R International* **31** (1992).
6. M. Büchler, H.-G. Schöneich, F. Stalder, " Discussion of Criteria to Assess the Alternating Current Corrosion Risk of Cathodically Protected Pipelines", in Joint technical meeting on pipeline research, p. Proceedings Volume Paper 26, PRCI, (2005).
7. L. V. Nielsen, B. Baumgarten, P. Cohn, "On-site measurements of AC induced corrosion: Effect of AC and DC parameters", in CEOCOR international Congress, CEOCOR, c/o C.I.B.E., Brussels, Belgium, (2004).
8. L. V. Nielsen, B. Baumgarten, P. Cohn, "Investigating AC and DC stray current corrosion", in CEOCOR international Congress, . Editor. CEOCOR, c/o C.I.B.E., Brussels, Belgium, (2005).
9. M. Büchler, F. Stalder, H.-G. Schöneich, "Eine neue elektrochemische Methode für die Ermittlung von Wechselstromkorrosion", *3R International* **44**, 396 (2005).
10. M. Büchler, C.-H. Voûte, H.-G. Schöneich, "Die Auswirkung des kathodischen Schutzniveaus. Diskussion des Wechselstromkorrosionsmechanismus auf kathodisch geschützten Leitungen: Die Auswirkung des kathodischen Schutzniveaus", *3R International* **47** 6(2008).
11. M. Büchler, C.-H. Voûte, H.-G. Schöneich, "Discussion of the mechanism of a.c.-corrosion of cathodically protected pipelines: The effect of the cathodic

- protection level", in CEOCOR international Congress, . Editor. CEOCOR, c/o C.I.B.E., Brussels, Belgium, (2008).
12. M. Büchler, C.-H.Voûte, "Wechselstromkorrosion an kathodisch geschützten Rohrleitungen: neue Erkenntnisse zum Mechanismus", *DVGW - energie/wasser-praxis* **6**, 18 (2009).
  13. M. Büchler, "Alternating current corrosion of cathodically protected pipelines: Discussion of the involved processes and their consequences on the critical interference values", *Materials and Corrosion* **63**, 1181 (2012).
  14. B. Leutner, S. Losacker, G. Siegmund, "Neue Erkenntnisse zum Mechanismus der Wechselstromkorrosion", *3R International* **37**, 135 (1998).
  15. M. Büchler, H.-G. Schöneich, "Investigation of Alternating Current Corrosion of Cathodically Protected Pipelines: Development of a Detection Method, Mitigation Measures, and a Model for the Mechanism", *Corrosion* **65**, 578 (2009).
  16. M. Büchler, C.-V.Voûte, H.-G. Schöneich, "Evaluation of the effect of cathodic protection levels on the a.c. corrosion on pipelines", Eurocorr Conference Proceedings, (2007).
  17. M. Büchler, "Kathodischer Korrosionsschutz: Diskussion der grundsätzlichen Mechanismen und deren Auswirkung auf Grenzwerte", *3R International* **49**, 342 (2010).
  18. M. Büchler, "Cathodic protection: A general discussion of the involved processes and their consequences for threshold values", in CEOCOR international Congress 2010 Bruges, CEOCOR, c/o VIVAQUA., Brussels, Belgium, (2010).
  19. M. Büchler, D. Joos, C.-H.Voûte, "Feldversuche zur Wechselstromkorrosion", *DVGW - energie/wasser-praxis* **Juli/August 2010**, 8 (2010).
  20. N. Kioupis, "Corrosion of buried pipelines detected on ER-probes", in CEOCOR international Congress 2011 Menthon-Saint-Bernard CEOCOR, c/o SYNERGRID, Brussels, Belgium, (2011).
  21. M. Büchler, "Strategien für die Optimierung des kathodischen Korrosionsschutzes von Rohrleitungen unter Wechselfspannungsbeeinflussung", *3R International*, 450 (2012).
  22. L. V. Nielsen, "AC corrosion criteria", in CEOCOR Workshop on the implementation of EN 15280, (November 2012).
  23. I. Ibrahim *et al.*, "On the mechanism of ac assisted corrosion of buried pipelines and its cp mitigation", in IPC2008, p. 64380, ASME, (2008).
  24. S. Goidanich, L. Lazzari, M. Ormollese, "AC interference effects on polarised steel", in CEOCOR 6th international Congress, CEOCOR, c/o C.I.B.E., Brussels, Belgium, (2003).
  25. L. V. Nielsen, "Considerations on measurements and measurement techniques under ac interference conditions", in CEOCOR international Congress 2011 Menthon-Saint-Bernard CEOCOR, c/o SYNERGRID, Brussels, Belgium, (2011).
  26. M. Pourbaix, "Atlas of electrochemical equilibria in aqueous solutions". (NACE, Houston, TX, 1974).



27. M. Büchler, P. Schmucki, H. Böhni, "Formation and Dissolution of the Passive Film on Iron studied by a Light Reflectance Technique", *J. Electrochem. Soc.* **144**, 2307 (1997).
28. P. Schmucki *et al.*, "Passivity of Iron in Alkaline Solutions Studied by In Situ XANEX and a Laser Reflection Technique", *J. Electrochem. Soc.* **6**, 2097 (1999).
29. Private communication with various pipeline operators